ACS OMEGA

Open Access



http://pubs.acs.org/journal/acsodf

Article

# Catalytic Aquathermolysis of Emulsified Residual Oils with Naphthenates

Xiaoyan Yu, Xiaolong Zhou,* Hongbo Jiang,* Ning Wang, Yichao Hu, and Tao Yu

Cite This: *ACS Omega* 2024, 9, 17681−17690

Read Online

ACCESS | Metrics & More | Article Recommendations

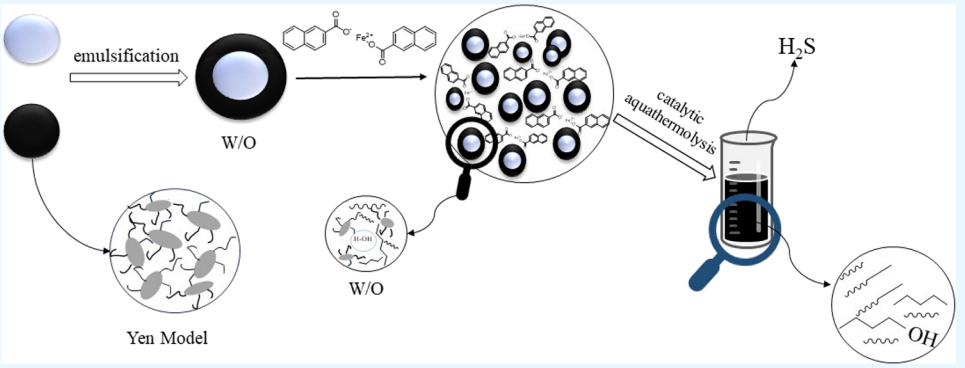


**ABSTRACT:** Catalytic aquathermolysis, a crucial aspect of chemical reutilization, converts the heavy components (such as resins and asphaltenes) of residual oil into lighter components. The use of transition-metal-based catalysts accelerates aquathermolysis reactions. It was observed that iron naphthenate exhibited greater efficiency for residual oils compared to manganese naphthenate and zinc naphthenate. Furthermore, the catalytic aquathermolysis of emulsified residual oil with iron naphthenate demonstrated an outstanding catalytic performance. Under the reaction conditions of 340 °C, 3 MPa, and 2 h, there was a remarkable decrease in viscosity and sulfur content of residual oil by 85.0 and 50.01%, respectively. Additionally, the alterations in the components of residual oils before and after aquathermolysis were examined through a four-component analysis and elemental analysis.

## 1. INTRODUCTION

Fossil fuels are expected to remain the predominant source of global energy for many decades due to their exceptional quality.[1−4] Countries worldwide are placing high expectations on the advanced processing and treatment of oil and gas resources, as well as the recycling of byproducts, to meet the growing demands associated with economic development and technological progress.[5−8] Residual oil, a byproduct of petroleum refining, poses challenges with a large density, high viscosity, elevated sulfur content, and poor mobility. Transporting residual oil is difficult, making the reduction of viscosity and desulfurization crucial,[9] especially for its potential use in blending marine fuel oil.[10−13]

Various methods, such as heating, mixing with thin oil, using soluble viscosity-reducing agents, emulsification, ultrasonics, and microbial processes, are currently employed to decrease the viscosity of residual oil.[14−18] However, these methods have limitations, including suboptimal viscosity reduction effects, high energy consumption, elevated costs, and concerns about secondary pollution.[9] In contrast, the catalytic aquathermolysis method is gaining widespread attention due to its advantages of simple equipment, ease of operation, low cost, and environmental friendliness.

The term "aquathermolysis," coined by Hyne et al., refers to thermal cracking in the presence of water.[19] This chemical reaction primarily breaks down the C−S bond, reducing the viscosity of the heavy crude oil. Even a slight fraction of bond breakage can significantly enhance the flow properties of heavy crude oils. Organosulfur compounds in heavy oil undergo a complex sequence of steps during aquathermolysis, as elucidated by Ancheyta[19,20] and colleagues, who developed a hydrolysis kinetic model based on their understanding of the reaction mechanism. The authors[5] highlighted the influence of operating conditions on aquathermolysis reactions and emphasized the need for further research on actual heavy oils to better comprehend the catalytic reaction mechanism and develop more accurate kinetic models.

**Received:** February 29, 2024
**Revised:** March 29, 2024
**Accepted:** April 1, 2024
**Published:** April 8, 2024

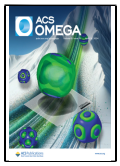

In the realm of aquathermolysis, the effectiveness of desulfurization and viscosity reduction is notably impacted by the involvement of transition metal (TM) catalysts. As far back as 1997, Weissman and colleagues highlighted the advantageous role of additional catalysts in facilitating sulfur removal.[21] Hyne and Clark, among others, have also emphasized the positive influence of catalysts based on transition metals (TMs) on aquathermolysis processes[22−24] and first proposed that water-soluble TM salts ($FeSO_4$, $RuCl_3$, $NiSO_4$, etc.) could accelerate the decomposition of S-containing components in heavy crude oil to alkane, carbon dioxide, hydrogen, and hydrogen sulfide, naturally leading to viscosity reduction. And for Loathe heavy crude oil, heavy components decreased and the light components increased simultaneously with the vanishment of heteroatoms (S, N)-containing compounds, leading to viscosity reduction efficiencies of 15−75% at 240 °C for 24 h with the inorganic TM salts.[25] Zhong et al.[26,27] found that the incorporation of Fe(II) salts and tetralin could provide a viscosity reduction up to 90% at 240 °C for 72 h. Compared with water-soluble inorganic TM salts, oil-soluble TM salts have the potential to provide better catalytic efficacy for reducing the viscosity of heavy crude oil by providing more effective interaction with the oil phase. In principle, the oil-soluble organic ligands are capable of improving the lipophilicity of the catalysts for bringing the TM ions to the surface and even internal of the heavy oil phase, thereby adequately facilitating the catalytic efficiency of TM ions. Several types of oil-soluble organic TM compounds, including TM carboxylates, involve alkyl carboxylates (or their mixture), oleates and naphthenates, TM sulfonates, and so on. By the selection of ligands with different molecular features and electronic structures, improved catalytic efficiencies could be achieved. In particular, some functional ligands may also serve as hydrogen donor to stimulate the desulfurization and hydrocracking process.[21] Liu et al.[28] found that 0.5 wt % addition of Mo(VI) oleate combined with a 0.1 wt % dose of surfactant at 200 °C and 5 MPa for 24h can result in the viscosity decrease of more than 90%. Liu et al.[29] prepared an Co(II) carboxylate by ion-exchange of $CoCl_2$ and 2-ethylhexanoic acid sodium salt. The catalytic aquathermolysis (280 °C for 24 h in 8−10 MPa $N_2$ atmosphere) could reduce the viscosity of heavy crude oil by 89.5%. Liu et al.[30] showed that adding 0.1 wt % of Ni(II) naphthenate at 280 °C for 24 h in an 8.1 MPa $N_2$ atmosphere could result in a viscosity reduction of 64.5%. Petrukhina et al.[31] compared Ni naphthenate, Co naphthenate, and Fe naphthenate for heavy crude oil recovery, respectively, with 0.1 wt % catalyst dosage. Viscosity reduction efficiencies of 20−78% can be obtained under controlled catalytic aquathermolysis condition (180−300 °C, 6−72 h) incorporation with 6 wt % dosage of tetralin as hydrogen donor. It was discovered by comparing the results of the studies mentioned above that TM naphthenates have more effective catalytic abilities and that the cyclic structure of the ligands provides more efficient interfacial interaction between the catalysts and the nonhydrocarbon components. More importantly, naphthenate may keep alkyl radicals from copolymerizing, which is essential for the synthesis of light components and is produced during pyrolysis. Nevertheless, one of the main obstacles preventing catalytic aquathermolysis from being used in the industry presently is the lengthy reaction time. Because of the water and oil insolubility, the system's oil−water contact surfaces are positively tiny, which substantially reduces the effectiveness of the catalytic aquathermolysis technologies currently. The easiest and most feasible, affordable, and efficient physical approach is emulsification.[32−34]

Emulsification is a convenient, simple, inexpensive, and effective physical method to upgrade oils for mixing others as a fuel.[35,36] The addition of an emulsifier into two immiscible streams (e.g., water and oil) with the help of agitation is an essential step to implement emulsification.[36,37] Li et al.[38] discovered that the synthesized polymers with higher HLB values exhibited excellent emulsifying properties for Shengli heavy oils. Hao Ma synthesized amphiphilic terpolymers (PAA and PAP) via homogeneous polymerization and compounded them with surfactant (SDS) to form different SP systems to reduce heavy oil viscosity. It was found that the solution viscosity is positively correlated with the emulsifying stability, and the SDS and PAP molecules could adsorb to the phase interface with asphaltene and naphthenic acid. Notwithstanding the significant progress already made in the emulsification and viscosity reduction of heavy crude oil with relevant experimental work, the application of emulsification approaches for catalytic aquathermolysis is still unclear.

In this study, we compared the catalytic effects of various TM naphthenates. Iron naphthenate demonstrated superior catalytic performance compared to zinc and manganese naphthenate, and as the reaction time was extended to 24 h, the viscosity reduction could reach up to 75.91%. At this time, the temperature and pressure are 340 °C and 3 MPa, respectively. Under the reaction conditions of 340 °C, 3 MPa, and 2 h, the viscosity reduction rate can reach 81.76%, and the desulfurization rate can reach 50.10% by emulsifying residual oil.

## 2. EXPERIMENT

**2.1. Characterization of Oil Sample.** Residual oil underwent a comprehensive four-component analysis, focusing on saturate, aromatic, resin, and asphaltene components, commonly abbreviated as SARA. This analysis was conducted using column chromatography[39] employing a column packed with neutral alumina (100−200 mesh) sourced from Bohr Chemical Reagents. The separation of SARA components was achieved through the utilization of various solvents, including toluene, *n*-heptane, and ethanol.

These solvents had a purity of 99% and were from Macklin. The four-component separation process of residual oil is shown in Figure 1.

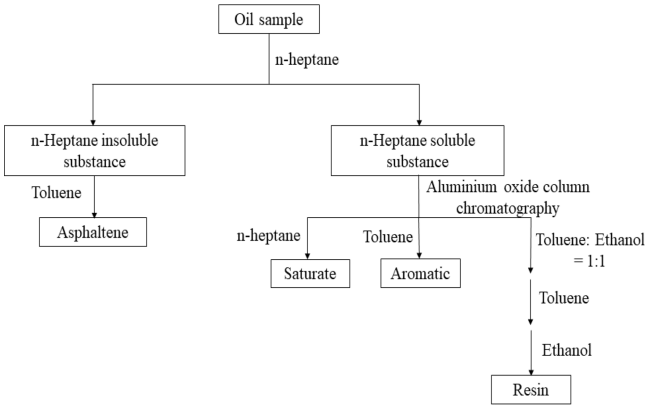


**Figure 1.** Flowchart of the four-component separation of oil samples.



https://doi.org/10.1021/acsomega.4c02022
ACS Omega 2024, 9, 17681−17690

*2.1.1. Elemental Analysis.* An elemental analyzer (ELEMENTAR VARIO EL CUBE) was used to determine the elemental composition (C, H, N, and S) of the residual oils before and after catalytic aquathermolysis.[4,40] X-ray photoelectron spectroscopy (Thermo Scientific K-Alpha) was used to analyze the oil samples' sulfur contents.[41] An inductively coupled plasma atomic emission spectrometer (Agilent) was used for determining other trace metal components, such as Ni, V, etc., in the residual oils.

*2.1.2. $^1H$ NMR.* Using a Bruker 400 MHz nuclear magnetic resonance spectrometer and $CDCl_3$ as the solvent, the spectra of oil samples containing resins and asphaltenes were determined. The fundamental average structures of the resins and asphaltenes were then deduced by analyzing the species of hydrogen atoms in the samples.[39,42]

*2.1.3. Gel Permeation Chromatography.* A Waters 1515 apparatus, which was used to deduce the fundamental average structure of resins and asphaltenes, was used to calculate the average molecular weight.[39]

**2.2. Emulsification of Residual Oil before Reaction.** An oil−water high-speed shear homogeneous emulsification apparatus was used for residual oil emulsification. First, the stabilizer, coemulsifier, and emulsifier were quantitatively dissolved in distilled water in the required proportions. The residual oil was subsequently heated to 80 °C and added gradually to the solution mentioned above. Then, the mixture was stirred violently for 20 min at 5000 rpm. Span 60 (CP), sodium oleate (65−90% oleic acid), *n*-butanol (AR), and triethanolamine (GC) were used in the emulsification.

**2.3. Catalytic Aquathermolysis.** Naphthenates, such as iron naphthenate (10% Fe), zinc naphthenate (8% Zn), and manganese naphthenate (6% Mn), were used as aquathermolysis catalysts.

The aquathermolysis experiments were conducted in an autoclave with a quartz tube (200 mL). Experimental studies used quartz tubes to avoid direct contact of oil samples with reactor walls. In this way, any catalytic effect of metals present on the inner walls of the reactor can be avoided. The system was evacuated with $N_2$ after adding the catalyst and emulsified residual oils to the quartz tube. The reaction temperature, pressure, oil/water ratio, catalyst dose, and reaction time were all adjusted, and the viscosity and sulfur content were measured both before and after the reaction.

## 3. RESULTS AND DISCUSSION

**3.1. Residual Oil Characterization.** The molecular structure of resins and asphaltenes was determined utilizing the enhanced Brown−Ladner technique. This approach incorporated the analysis of the elemental composition, average molecular weight, and $^1H$ nuclear magnetic resonance (NMR) spectroscopy. Furthermore, Table 2 provides the ratios of the various types of hydrogens identified in the analysis.

$C_T$ and $H_T$ are the total amounts of carbon and hydrogen, respectively, and the $H_T$ is the ratio of carbon to hydrogen calculated with eq 1.[39] The aromaticity ($A$) and aromatic condensation index ($H_{AU}/C_A$) of the resins and asphaltenes were calculated with eqs 2 and 3.[39] The lower the aromatic condensation is, the higher is the $H_{AU}/C_A$ ratio. The average structural parameters of oil samples of resins and asphaltenes were analyzed (Tables 1 and 2), and it was discovered that sulfur and nitrogen contents were mainly present in resins and asphaltenes; in comparison to asphaltenes, resins had a larger relative content of H, a smaller relative content of C, a larger H/C ratio, a smaller relative content of C, and a smaller degree of condensation. The model parameters were based on the molecular average structure of the resins' and asphaltenes' combined elements. And the structural parameters, combined with the modified Yen model,[43] can provide the foundation for the subsequent mechanistic examination.

**Table 1. Main Characteristics of the Initial Residual Oil**

| composition and properties | value |
|---|---|
| viscosity at 100 °C (mPa·s)[a] | 8787 |
| density at 25 °C (g·cm$^{-3}$) | 0.972 |
| SARA fractions (%) | |
| saturates | 23.67 |
| aromatics | 37.62 |
| resins | 32.59 |
| asphaltenes | 6.12 |
| elemental analysis (wt %) | |
| carbon | 85.96 |
| hydrogen | 9.975 |
| sulfur | 1.824 |
| nitrogen | 0.81 |
| nickel | 0.009 |
| vanadium | 0.065 |

[a]Viscosity was measured by a Brookfield NDJ-1C Rotational Viscometer at 100 °C.

**Table 2. Mean Structural Parameters of Resin and Asphaltene**

| sample | asphaltene | resin |
|---|---|---|
| C (wt %) | 84.555 | 83.595 |
| H (wt %) | 9.988 | 7.038 |
| S (wt %) | 2.072 | 2.844 |
| N (wt %) | 1.43 | 1.755 |
| $N_H/N_C$[a] | 1.417 | 1.01 |
| $H_\alpha$ (%)[b] | 10.4 | 6.3 |
| $H_\beta$ (%)[c] | 7.5 | 55 |
| $H_\gamma$ (%)[d] | 62.2 | 29.5 |
| $H_A$ (%)[e] | 19.9 | 9.2 |
| $H_{AU}/C_A$ | 0.537 | 0.228 |
| $R_T$ | 82.25 | 178.42 |
| $R_A$ | 63.15 | 141.05 |
| $R_N$ | 19.11 | 37.37 |
| $C_T$[f] | 725 | 784 |
| $C_A$[f] | 268.488 | 427.156 |
| $C_N$[f] | 76.425 | 112.11 |
| $C_P$[f] | 380.087 | 244.734 |
| $f_A$[g] | 0.37 | 0.55 |
| $f_N$[g] | 0.11 | 0.14 |
| $f_P$[g] | 0.52 | 0.31 |

[a]$N_H/N_C$ is the atomic ratio of hydrogen to carbon. [b]$H_\alpha$ stands for aliphatic hydrogen on $C_\alpha$ to aromatic rings. [c]$H_\beta$ stands for the $CH_2$, CH hydrogen on $C_\beta$ and carbons beyond $C_\beta$, $CH_3$ hydrogen on $C_\beta$, and $CH_2$, CH hydrogen on alkanes. [d]$H_\gamma$ stands for the $CH_3$ hydrogen on $C_\gamma$ and beyond $C_\gamma$, and $CH_3$ hydrogen on alkanes. $R_T$, $R_A$, and $R_N$ represent the total ring number, aromatic ring number, and naphthenic ring number, respectively. [e]$H_A$ stands for aromatic hydrogen. [f]$C_T$, $C_A$, $C_N$, and $C_P$ represent the total carbon number, aromatic carbon number, naphthenic carbon number, and paraffinic carbon number, respectively. [g]$f_A$, $f_N$, and $f_P$ are the ratio of aromatic carbon, naphthenic carbon, and paraffinic carbon, respectively.



https://doi.org/10.1021/acsomega.4c02022
ACS Omega 2024, 9, 17681−17690

$$H_T = H_\alpha + H_\beta + H_\gamma + H_A \quad (1)$$

$$f_A = \frac{C_T/H_T - (H_\alpha + H_\beta + H_\gamma/2H_T)}{C_T/H_T} \quad (2)$$

$$\frac{H_{AU}}{C_A} = \frac{H_A/H_T + H_\alpha/2H_T}{C_T/H_T - (H_\alpha + H_\beta + H_\gamma/2H_T)} \quad (3)$$

The electronegativity of atoms within a chemical bond plays a crucial role in determining the variations in electronic binding energies observed in X-ray photoelectron spectroscopy (XPS) spectra (refer to Figure 2). In this context, the same

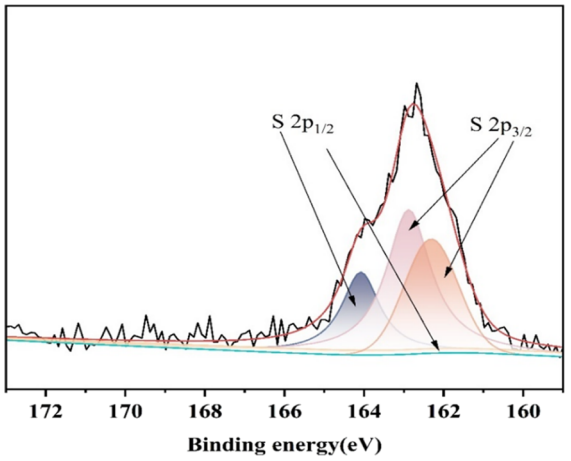


**Figure 2.** XPS spectra of S in the residual oil.

atom can display distinct chemical shifts, which are contingent upon the chemical composition of its surrounding environment. Consequently, XPS offers a valuable means to analyze the presence and distribution patterns of sulfur species in residual oil. The usual binding energy of thiophene-type sulfur is 164−165 eV, whereas that of thioether and disulfide is 163−164 eV. Two spectral peaks with a theoretical peak area ratio of 2, $Sp_{3/2}$ and $Sp_{1/2}$, represent the p-electron response of the S in the XPS spectrum. A 1.2 eV gap[44,45] should exist between the peaks. The peaks in the XPS spectra were divided by the electron binding energies of the many forms of S that are known to exist, and the integral value of each peak area was output. The normalization calculation approach may be used to do a quantitative analysis of the existing forms of S components and their respective proportions. According to the fitting outcomes, thioether and thiophene make up the majority of the sulfur compounds in residual oil, with thioether accounting for 38.68% of the total sulfur content and thiophene accounting for 61.32%.

**3.2. Comparison of Different Catalysts.** Through a comparative analysis of the catalytic performance, manganese naphthenate, iron naphthenate, and zinc naphthenate were evaluated to identify the most suitable catalyst for catalytic aquathermolysis. Figure 3 illustrates that zinc naphthenate exhibited minimal catalytic performance, whereas iron naphthenate demonstrated the most favorable results, achieving a remarkable viscosity reduction rate of up to 81.76%. Manganese naphthenate ranked second, with a viscosity reduction rate reaching 41.49%. Additionally, with manganese naphthenate, an inflection point was observed around 310 °C. Beyond this temperature, the formation of black solids at the

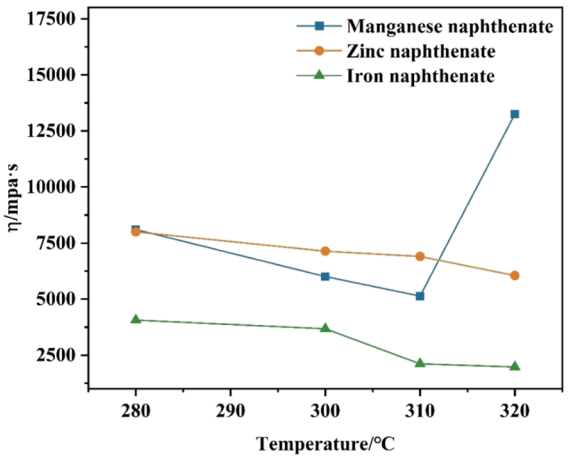


**Figure 3.** Viscosity with different catalysts of catalytic aquathermolysis (reaction conditions: 3 MPa, 24 h, oil−water ratio: 7:3, catalyst dosage 2 wt %).

bottom indicated a shift toward coking reactions, attributed to the dominance of the polymerization process.

Further analysis in Figure 4 revealed that iron naphthenate consistently outperformed manganese naphthenate under

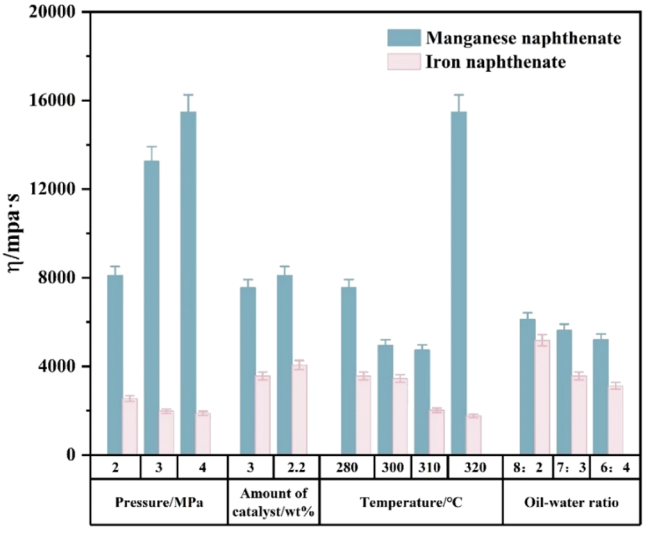


**Figure 4.** Viscosity with iron naphthenate and manganese naphthenate under different conditions of catalytic aquathermolysis.

various reaction conditions. Given its superior catalytic performance, iron naphthenate was selected as the catalyst for subsequent aquathermolysis experiments. Figure 5 demonstrates a gradual improvement in iron naphthenate's catalytic performance as the reaction time is extended.

In view of the economic and practical aspects of industrial operations, a reaction time of 2 h was selected. This choice not only contributes to cost savings in terms of industrial equipment investments but also attains the desired viscosity reduction of 54.89% in the residual oil.

**3.3. Effect of Residual Oil Emulsification on Aquathermolysis.** Figure 6 contrasts the effects of aquathermolysis reactions on residual oil, comparing emulsified oil with two different emulsifiers to nonemulsified oil. The results highlight that emulsification plays a significant role in facilitating the smooth progress of the reaction. Sodium oleate, in particular,


https://doi.org/10.1021/acsomega.4c02022
ACS Omega 2024, 9, 17681−17690

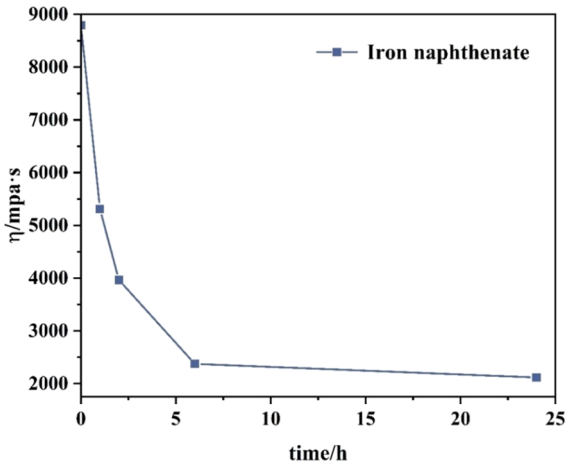


**Figure 5.** Viscosity with iron naphthenate under different reaction times of catalytic aquathermolysis (reaction conditions: 3 MPa, 320 °C, oil−water ratio: 7:3, catalyst dose 2 wt %).

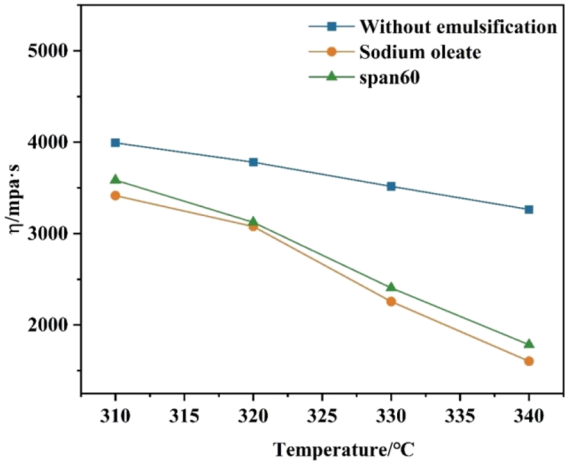


**Figure 6.** Viscosity of aquathermolysis with emulsification and without emulsification (reaction conditions: 3 MPa, 2 h, oil−water ratio: 7:3, emulsifier dosage 1 wt %).

demonstrates superior emulsification capabilities and enhanced viscosity reduction in the temperature range of 310 to 340 °C compared to Span 60. The graph also illustrates that at 320 °C, both Span 60 and sodium oleate reach an inflection point in their emulsification impact, and as the temperature increases further, viscosity reduction occurs gradually. This suggests that sodium oleate enhances the oil−water interaction, facilitating complete contact between residual oil and water and thereby expediting the reaction.

Co-emulsifiers play a crucial role in regulating the hydrophilic−lipophilic balance (HLB) of the emulsifier and contribute to the formation of smaller droplets, thereby enhancing emulsion stability.[46,47] Short-chain alcohols or nonionic surfactants with suitable HLB values are often employed as coemulsifiers. Examples include *n*-butanol, ethylene glycol, ethanol, propylene glycol, glycerol, and polyglycerol esters.

Furthermore, the stabilizer used in the emulsification process also influences the stability of the emulsion to a certain extent. Triethanolamine is a common stabilizer utilized in emulsification reactions. Its role is to maintain the stability of emulsion components, preventing delamination or degradation and contributing to the overall robustness of the emulsion.

In Figure 7, it is evident that the addition of both *n*-butanol and triethanolamine plays a beneficial role in the emulsification

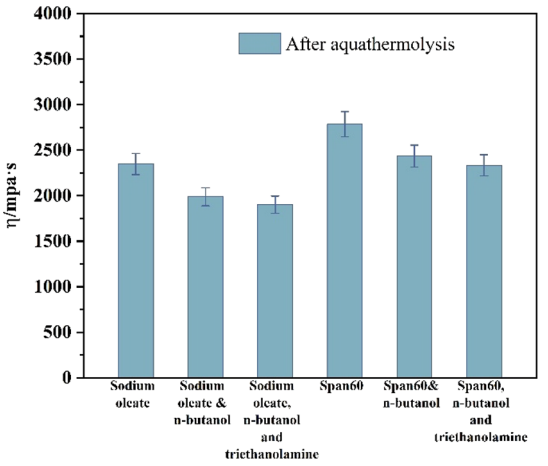


**Figure 7.** Viscosity of aquathermolysis with emulsifiers and coemulsifiers (reaction conditions: 3 MPa, 2 h, 330 °C, oil−water ratio: 7:3).

reaction, significantly promoting the viscosity reduction in the aquathermolysis process. The graph illustrates that augmenting the emulsifier quantity has a substantial positive impact on the aquathermolysis reaction. However, the presence or absence of triethanolamine does not seem to affect the associated viscosity. Moreover, there is a 4.36% increase in the viscosity reduction rate when the emulsifier dosage is doubled (Table 3).

**Table 3. Viscosity of Aquathermolysis with Different Amounts of Emulsifier (Reaction Conditions: 340 °C, 2 h, Oil−Water Ratio 7:3, *n*-Butanol: 0.5 wt %)**

| amount of emulsifier/wt % | viscosity/mPa·s (100 °C) |
|---|---|
| 0.5 | 1987 |
| 1.0 | 1604 |
| 1.5 | 1487 |
| 2.0 | 1326 |

Although the aquathermolysis reaction can be enhanced by adding more emulsifier, it is important to note that the viscosity decrease is not directly proportional to the industrial cost, leading to potential emulsifier waste. Table 4 highlights that the process can be more effective with increased water addition, resulting in a significant viscosity reduction. However, caution is advised against indiscriminate increases

**Table 4. Viscosity of Aquathermolysis with Different Oil−Water Ratios (Reaction Conditions: 340 °C, 2 h, Sodium Oleate: 0.5 wt %, *n*-Butanol: 0.5 wt %)**

| oil−water ratio | viscosity/mPa·s (100 °C) |
|---|---|
| 7:3 | 1987 |
| 8:3 | 2134 |
| 9:3 | 2289 |
| 10:3 | 2354 |



https://doi.org/10.1021/acsomega.4c02022
ACS Omega 2024, 9, 17681−17690

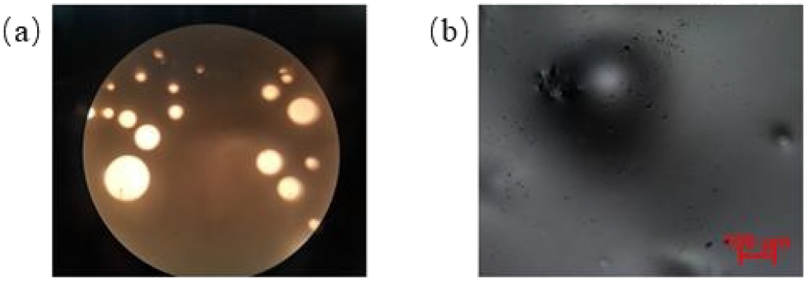


**Figure 8.** Emulsifying state: (a) optical microscope and (b) polarizing microscope.

in water content due to the associated costs of equipment, water supply, and additional water treatment.

In Figure 8, the W/O (water-in-oil) emulsion mixture formed by residual oil and water, under the influence of the emulsifier and high-speed shear force, is depicted. This process leads to the reduction of residual oil into micron-sized small molecules.

**3.4. Effect of Emulsification on Catalytic Aquathermolysis with Iron Naphthenate.** By examination of Tables 5−7 along with Figure 9, it becomes evident that the reaction viscosity experiences a decrease as the catalyst dosage increases. Additionally, the viscosity tends to decrease initially with a rise in reaction pressure and further decreases with an increase in temperature.

**Table 5. Viscosity of Catalytic Aquathermolysis with Different Amounts of Catalyst (Reaction Conditions: 340 °C, 2 h, Oil−Water Ratio 10:3, Sodium Oleate: 0.5 wt %, *n*-Butanol: 0.5 wt %)**

| amount of catalyst/wt % | viscosity/mPa·s (100 °C) |
|---|---|
| 3 | 1589 |
| 2 | 2006 |
| 1 | 2077 |
| 0.5 | 2354 |
| 0 | 3109 |

**Table 6. Viscosity of Catalytic Aquathermolysis with Iron Naphthenate under Different Initial Pressures (Reaction Conditions: 340 °C, 2 h, Oil−Water Ratio 10:3, Sodium Oleate: 0.5 wt %, *n*-Butanol: 0.5 wt %, Iron Naphthenate: 1 wt %)**

| pressure/MPa | viscosity/mPa·s (100 °C) |
|---|---|
| 3 | 2077 |
| 2 | 2111 |

**Table 7. Viscosity of Catalytic Aquathermolysis with Iron Naphthenate under Different Reaction Temperatures (Reaction Conditions: 3 MPa, 2 h, Oil−Water Ratio 10:3, Sodium Oleate: 0.5 wt %, *n*-Butanol: 0.5 wt %, Iron Naphthenate: 1 wt %)**

| temperature/°C | viscosity/mPa·s (100 °C) |
|---|---|
| 300 | 4866 |
| 310 | 4722 |
| 320 | 3947 |
| 330 | 2396 |
| 340 | 2111 |

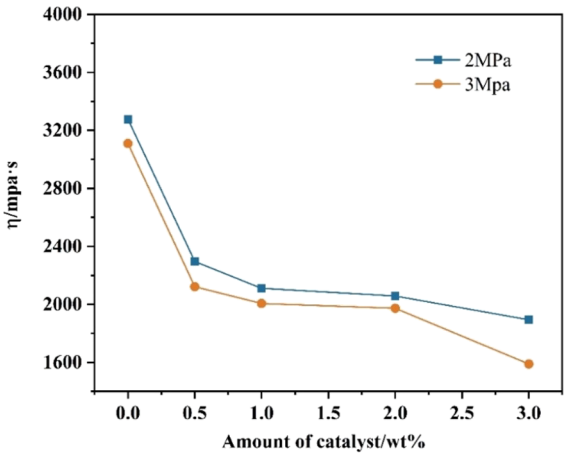


**Figure 9.** Copromoting effect of iron naphthenate addition and initial reaction pressure(reaction conditions:340 °C, 2 h, oil−water ratio 10:3, sodium oleate: 0.5 wt %, *n*-butanol: 0.5 wt %).

The increase in emulsification, which enhances the oil−water contact area, allows water to optimize its action and leads to viscosity reduction. A similar reduction in viscosity is observed when no catalyst is added, as indicated in Table 5. The viscosity progressively decreases with an increase in catalyst dosage, but an excess of catalyst tends to hinder the improvement of the reaction's efficiency, causing a decrease in catalytic reaction efficiency. At a catalyst dosage of 3 wt %, the catalytic effect still increases significantly; however, the excessive use of catalyst leads to increased raw material costs. Furthermore, considering the metal content in the catalyst, excessive use can result in an elevated content of metal components in the residual oil. Because oil-soluble catalysts are not recovered, metal components persist in the oil, which is unfavorable for the subsequent industrial use of residual oil.

Based on the analysis of the effects of different catalyst dosages and initial pressures on viscosity at the same temperature, it is observed that the rate of viscosity reduction in catalytic aquathermolysis at a 0.5 wt % catalyst dosage and 3 MPa initial pressure closely aligns with that at a 1.0 wt % catalyst dosage and 2 MPa initial pressure. The rates of viscosity reduction are 76.38 and 76.00%, respectively. Through a comparison with other data, it becomes evident that the initial pressure and the catalyst dosage collectively promote the reaction.

The viscosity undergoes a substantial reduction with an increasing reaction temperature, notably decreasing beyond 320 °C (refer to Table 7). This suggests that the catalytic efficacy of iron naphthenate is particularly pronounced within this temperature range. In comparison to the results of catalytic aquathermolysis of residual oil without emulsification, the


https://doi.org/10.1021/acsomega.4c02022
ACS Omega 2024, 9, 17681−17690

findings from this process indicate that the increased oil−water contact area resulting from emulsification can amplify the catalytic efficiency of catalytic aquathermolysis. Moreover, the temperature increases not only influence but also assist in establishing the dominant position of the hydrothermal reaction.

The results demonstrate that the temperature, initial pressure, and catalyst dosage all act as positive catalytic factors that collectively contribute to increased catalytic activity. Therefore, optimizing both the industrial cost and catalytic efficiency can be achieved by adjusting the interplay between two or three factors: temperature, initial pressure, and catalyst dosage.

**3.5. Characterization before and after Reaction.** Table 8 illustrates that iron naphthenate is effective in promoting the conversion of heavy components in residual oil to lighter components. During catalytic aquathermolysis with iron naphthenate, the contents of asphaltene and resin decrease, whereas the contents of saturate and aromatic increase.

**Table 8. Changes of Components before and after Reaction of Residual Oils**

| oil sample | saturate | aromatic | resin | asphaltene |
|---|---|---|---|---|
| before reaction | 23.67 | 37.62 | 32.59 | 6.12 |
| after reaction | 29.53 | 40.98 | 25.00 | 4.49 |

In Table 9, the elemental compositions and NH/NC ratios of several residual oils before and after catalytic aquathermolysis with iron naphthenate are presented. Under the conditions of 340 °C, 3 MPa, and an oil-to-water ratio of 10:3, the most pronounced catalytic effect is observed when using 1 wt % sodium oleate and 0.5 wt % *n*-butanol. Throughout the reaction, the N content decreased from 0.81 to 0.78, the S content decreased from 1.824 to 0.90, and the $N_H/N_C$ ratio (atomic ratio of hydrogen to carbon) of the residual oil increased from 1.39 to 1.64.

These results suggest that during the catalytic aquathermolysis reaction, iron naphthenate may facilitate the breaking of macromolecular C−C and C−X (X = S, N, and O) bonds, leading to structural alterations and a decrease in viscosity and sulfur content of residual oil, ultimately enhancing its quality.

**3.6. The Mechanism of Catalytic Aquathermolysis with Iron Naphthenate.** The mass loss that occurs when iron naphthenate breaks down under a $N_2$ atmosphere is depicted in Figure 10. In the temperature range of 30 to 500 °C, the mass spectrometry data showed two significant, dramatic mass losses of iron naphthenate: the first mass loss was 46.06% at a temperature of approximately 123.2−246.7 °C, and the second mass loss was 47.45% at a temperature of approximately 364.2−397.1 °C. The figure also shows that at around 246.7−364.2 °C, the mass loss rate of iron naphthenate slows down and uniformly drops. The mass spectral data indicate that naphthenic acid's ligand pyrolyzes between 219 and 300 °C. The results of the mass spectrometry indicate that the naphthenic acid ligand undergoes pyrolysis at around 219−300 °C, producing a modest amount of light hydrocarbon gases. In the second step, which had a temperature range of 320 to 370 °C, the principal gaseous products were hydrogen and trace amounts of carbon dioxides and oxides.

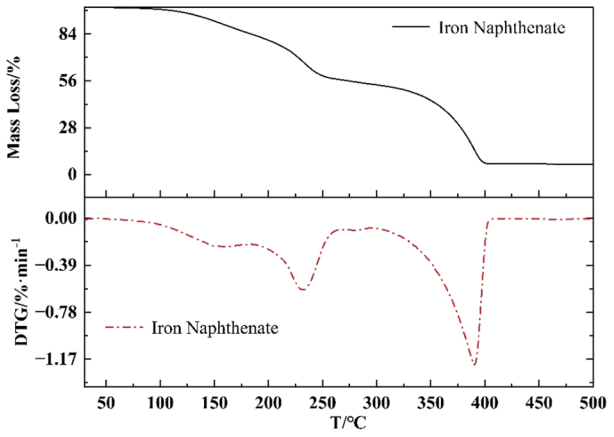


**Figure 10.** TG-DTG curves of iron naphthenate at a heating rate of 10 °C/min under a $N_2$ atmosphere.

From the emulsification perspective, high-speed shear force acts on residual oil and water, breaking them into micrometer-sized particles and forming a W/O (water-in-oil) emulsified mixture. This process increases the contact area between oil, water, and the catalyst, facilitating closer interactions among the three components. This sets a favorable precondition for the subsequent reaction.

Considering iron naphthenate, the catalytic activity is enabled by the naphthalene ring of the ligand naphthenic acid and the catalytic action of the transition metal Fe. In the early stages of the reaction, its organic ligand creates a conducive hydrogen atmosphere. However, as the reaction progresses and the temperature rises, the organic ligand of iron naphthenate undergoes pyrolysis. This transformation allows Fe to come into better contact with the oil/water mixture, promoting and enhancing the catalytic reaction.

The mechanism of action is depicted schematically in Figure 11, with the asphaltene model represented by a modified Yen

**Table 9. Elemental Changes of Residual Oil before and after Reaction[a]**

| oil sample | before reaction | [1#]after reaction 1 | [1#]after reaction 2 | [2#]after reaction 3 | [3#]after reaction 4 |
|---|---|---|---|---|---|
| temperature/°C | | 280 | 310 | 340 | 340 |
| pressure/MPa | | 3 | 3 | 3 | 3 |
| amount of catalyst/wt % | | 2.2 | 2.2 | 3 | 1 |
| time/h | | 24 | 1 | 2 | 2 |
| oil−water ratio | | 7:3 | 7:3 | 10:3 | 10:3 |
| $N_H/N_C$ | 1.39 | 1.42 | 1.40 | 1.64 | 1.64 |
| N | 0.81 | 0.8 | 0.8 | 0.75 | 0.78 |
| S | 1.82 | 1.70 | 1.78 | 0.91 | 0.9 |

[a]Note: 1# is nonemulsified residual oil, 2# is emulsified residual oil with 0.5 wt % sodium oleate and 0.5 wt % *n*-butanol, and 3# is emulsified residual oil with 1 wt % sodium oleate and 0.5 wt % *n*-butanol.



https://doi.org/10.1021/acsomega.4c02022
ACS Omega 2024, 9, 17681−17690

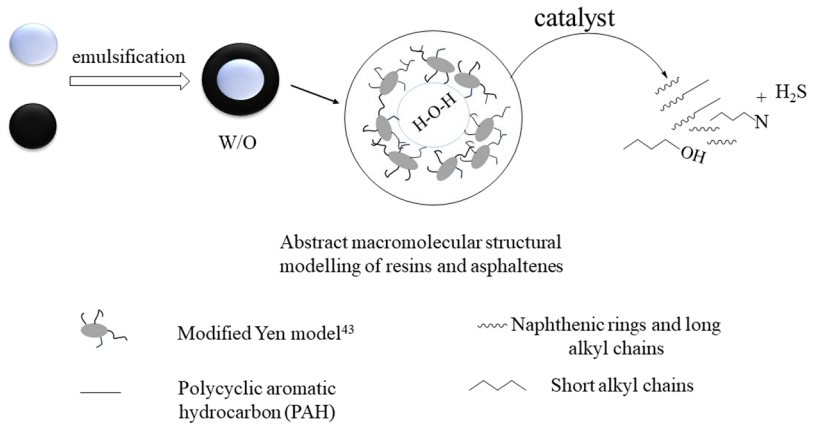


**Figure 11.** Reaction mechanism of catalytic aquathermolysis with iron naphthenate.

model.[43] Each gray circle signifies a single polycyclic aromatic hydrocarbon (PAH) disordered "stack" within a nanoaggregate. The crooked lines symbolize the peripheral alkane substituents of the nanoaggregate. The ring-structured naphthenic acids contribute to more efficient interfacial contact of the catalyst with the nonhydrocarbon constituents in heavy crude oil. More importantly, they have the capability of preventing the alkyl free radicals generated during pyrolysis processing from copolymerizing. This prevention is crucial for the synthesis of light components.[21]

## 4. CONCLUSIONS

In this study, the catalytic activity of various transition metal naphthenates as catalysts, along with the emulsification's stimulating influence on catalytic aquathermolysis, was investigated. Iron naphthenate has emerged as an outstanding catalyst for catalytic aquathermolysis. In the absence of an emulsification process, a 24 h reaction at 340 °C and 3 MPa pressure with 2 wt % iron naphthenate as a catalyst resulted in the most significant viscosity reduction of 75.91%. Iron naphthenate plays a role in reducing the likelihood of free radical collisions, inhibiting the polymerization stage, and facilitating the cleavage of C−S bonds, consequently reducing the sulfur content in residual oil. This leads to a reduction in viscosity accompanied by a decrease in resin and asphaltene concentration.

Residual oil was emulsified with sodium oleate and *n*-butanol to create a W/O (water-in-oil) emulsion mixture, effectively increasing the contact area of the oil, water, and catalyst. Under conditions of 340 °C, 3 MPa pressure, and an oil−water ratio of 10:3, the viscosity reduction and desulfurization rate were maximized, reaching 81.76 and 50.10%, respectively. The combination of emulsification and catalytic aquathermolysis holds significant industrial applicability value.

## AUTHOR INFORMATION


### Corresponding Authors

**Xiaolong Zhou** − *International Joint Research Center of Green Chemical Engineering, School of Chemical Engineering, East China University of Science and Technology, Shanghai 200237, China*; Email: xiaolong@ecust.edu.cn

**Hongbo Jiang** − *International Joint Research Center of Green Chemical Engineering, School of Chemical Engineering, East China University of Science and Technology, Shanghai 200237, China*; orcid.org/0000-0002-3025-682X; Email: hbjiang@ecust.edu.cn

### Authors

**Xiaoyan Yu** − *International Joint Research Center of Green Chemical Engineering, School of Chemical Engineering, East China University of Science and Technology, Shanghai 200237, China*; orcid.org/0009-0005-9434-4043

**Ning Wang** − *International Joint Research Center of Green Chemical Engineering, School of Chemical Engineering, East China University of Science and Technology, Shanghai 200237, China*; orcid.org/0009-0005-2870-7790

**Yichao Hu** − *International Joint Research Center of Green Chemical Engineering, School of Chemical Engineering, East China University of Science and Technology, Shanghai 200237, China*; orcid.org/0009-0009-3617-3898

**Tao Yu** − *International Joint Research Center of Green Chemical Engineering, School of Chemical Engineering, East China University of Science and Technology, Shanghai 200237, China*

Complete contact information is available at: https://pubs.acs.org/10.1021/acsomega.4c02022


### Notes

The authors declare no competing financial interest.

## ACKNOWLEDGMENTS

This research did not receive any specific grant from funding agencies in the public, commercial, or not-for-profit sectors.

## REFERENCES

(1) Djimasbe, R.; Varfolomeev, M. A.; Al-Muntaser, A. A.; Yuan, C.; Feoktistov, D. A.; Suwaid, M. A.; Kirgizov, A. J.; Davletshin, R. R.; Zinnatullin, A. L.; Fatou, S. D.; Galeev, R. I.; Rakhmatullin, I. Z.; Kwofie, M.; Klochkov, V. V.; Prochukhan, K. Y. Oil dispersed nickel-based catalyst for catalytic upgrading of heavy oil using supercritical water. *Fuel* **2022**, *313*, No. 122702.

(2) Dong, X.; Liu, H.; Chen, Z.; Wu, K.; Lu, N.; Zhang, Q. Enhanced oil recovery techniques for heavy oil and oilsands reservoirs after steam injection. *Applied Energy* **2019**, *239*, 1190−1211.

(3) Khafizov, N. R.; Madzhidov, T. I.; Yuan, C.; Varfolomeev, M. A.; Kadkin, O. N. Theoretical insight into the catalytic effect of transition metal ions on the aquathermal degradation of heavy oil: A DFT study of cyclohexyl phenyl amine cleavage. *Fuel* **2022**, *312*, No. 123002.

(4) Vakhin, A. V.; Aliev, F. A.; Mukhamatdinov, I. I.; Sitnov, S. A.; Sharifullin, A. V.; Kudryashov, S. I.; Afanasiev, I. S.; Petrashov, O. V.;

Nurgaliev, D. K. Catalytic Aquathermolysis of Boca de Jaruco Heavy Oil with Nickel-Based Oil-Soluble Catalyst. *Processes* **2020**, *8* (5), 532.
(5) Tirado, A.; Yuan, C.; Varfolomeev, M. A.; Ancheyta, J. Kinetic modeling of aquathermolysis for upgrading of heavy oils. *Fuel* **2022**, *310*, No. 122286.
(6) Khelkhal, M. A.; Lapuk, S. E.; Buzyurov, A. V.; Ignashev, N. E.; Shmeleva, E. I.; Mukhamatdinov, I. I.; Vakhin, A. V. Thermal Behavior of Heavy Oil Catalytic Pyrolysis and Aquathermolysis. *Catalysts* **2022**, *12* (4), 449.
(7) Ahmed, U.; Meehan, D. N. The Art of Data Mining and Its Impact on Unconventional Reservoir Development. In *Unconventional Oil and Gas Resources*, 2016; pp LaFollette, R. F.; Hughes, B.; Lou, X. L.; ConocoPhillips; Zhong, M.; Hughes, B.; eds. CRC Press.
(8) Wang, J.; Feng, L.; Steve, M.; Tang, X.; Gail, T. E.; Mikael, H. China's unconventional oil: A review of its resources and outlook for long-term production. *Energy* **2015**, *82*, 31−42.
(9) Huang, X.; Zhou, C.; Suo, Q.; Zhang, L.; Wang, S. Experimental study on viscosity reduction for residual oil by ultrasonic. *Ultrasonics Sonochemistry* **2018**, *41*, 661−669.
(10) Kapustin, N. O.; Grushevenko, D. A. Global prospects of unconventional oil in the turbulent market: a long term outlook to 2040. *Oil Gas Sci. Technol. − Rev. IFP Energies Nouvelles* **2018**, *73*, 67.
(11) Bilgili, L. Life cycle comparison of marine fuels for IMO 2020 Sulphur Cap. *Science of The Total Environment* **2021**, *774* (774), No. 145719.
(12) Chu Van, T.; Ramirez, J.; Rainey, T.; Ristovski, Z.; Brown, R. J. Global impacts of recent IMO regulations on marine fuel oil refining processes and ship emissions. *Transportation Research Part D: Transport and Environment* **2019**, *70*, 123−134.
(13) Mitra, S.; Racha, S. M.; Shown, B.; Mandal, S.; Das, A. K. New insights on oxidative desulfurization for low sulfur residual oil production. *Sustainable Energy Fuels* **2023**, *7*, 270−279.
(14) Chen, X.; Wang, N.; Xia, S. Research progress and development trend of heavy oil emulsifying viscosity reducer: a review. *Petroleum Science and Technology* **2021**, *39* (15−16), 550−563.
(15) Zhang, S.; Li, Q.; Xie, Q.; Zhu, H.; Xu, W.; Liu, Z. Mechanism Analysis of Heavy Oil Viscosity Reduction by Ultrasound and Viscosity Reducers Based on Molecular Dynamics Simulation. *ACS Omega* **2022**, *7* (41), 36137−36149.
(16) Li, X.; Zhang, F.; Liu, G. Review on new heavy oil viscosity reduction technologies. *IOP Conf. Ser.: Earth Environ. Sci.* **2022**, *983* (1), No. 012059.
(17) Dai, C.; Zhao, F., Viscosity Reduction of Heavy Oil. In *Oilfield Chemistry*, Dai, C.; Zhao, F., Eds. Springer Singapore: Singapore, 2018; pp 197−209.
(18) Zhu, J.; Li, C. X.; Yang, F.; Xin, P. G. Research progress in new viscosity-reducing techniques for heavy oil. *J. Xi'an Shiyou Univ., Nat. Sci. Ed.* **2012**, *27*, 64−70.
(19) Hyne, J. B.; Clark, P. D.; Clarke, R. A.; Koo, J.; Greidanus, J. W. Aquathermolysis of heavy oils. *Rev. Tec. INTEVEP* **1982**, *2:2*, 87.
(20) Maity, S. K.; Ancheyta, J.; Marroquín, G. Catalytic Aquathermolysis Used for Viscosity Reduction of Heavy Crude Oils: A Review. *Energy Fuels* **2010**, *24* (5), 2809−2816.
(21) Li, C.; Huang, W.; Zhou, C.; Chen, Y. Advances on the transition-metal based catalysts for aquathermolysis upgrading of heavy crude oil. *Fuel* **2019**, *257*, No. 115779.
(22) Clark, P. D.; Kirk, M. J. Studies on the Upgrading of Bituminous Oils with Water and Transition Metal Catalysts. *Energy Fuels* **1994**, *8* (2), 380−387.
(23) Clark, P. D.; Hyne, J. B. Steam-oil chemical reactions: Mechanisms for the aquathermolysis of heavy oil. *AOSTRA J. Res.* **1984**, *1*, 15−20.
(24) Clark, P. D.; Hyne, J. B.; Tyrer, J. D. Chemistry of organosulphur compound types occurring in heavy oil sands: 1. High temperature hydrolysis and thermolysis of tetrahydrothiophene in relation to steam stimulation processes. *Fuel* **1983**, *62* (8), 959−962.
(25) Fan, H.; Zhang, Y.; Lin, Y. The catalytic effects of minerals on aquathermolysis of heavy oils. *Fuel* **2004**, *83* (14), 2035−2039.
(26) Zhong, L. G.; Liu, Y. J.; Fan, H. F.; Jiang, S. J., Liaohe Extra-Heavy Crude Oil Underground Aquathermolytic Treatments Using Catalyst and Hydrogen Donors under Steam Injection Conditions. In *SPE International Improved Oil Recovery Conference in Asia Pacific*, SPE 2003; pp SPE-84863-MS.
(27) Jiang, S.; Liu, X.; Liu, Y.; Zhong, L., In Situ Upgrading Heavy Oil by Aquathermolytic Treatment Under Steam Injection Conditions. In *SPE International Symposium on Oilfield Chemistry*, SPE 2005; pp SPE-91973-MS.
(28) Liu, Y.; C, E.; Wen, S.; Liu, C. The preparation and evaluation of oil-soluble catalyst for aquathermolysis of heavy oil. *Chem. Eng. Oil Gas* **2005**, *34* (6), 511−2.
(29) Zhao, F.; Liu, Y.; Fu, Z.; Zhao, X. Using hydrogen donor with oil-soluble catalysts for upgrading heavy oil. *Russian Journal of Applied Chemistry* **2014**, *87* (10), 1498−1506.
(30) Liu, Y. J.; Zhao, F.; Zhao, G.; Hu, S. B.; Lin, Z. Study on Upgrading Heavy Oil by Catalytic Aquathermolysis Using Formic Acid as Hydrogen Donor. *Oilfield Chem.* **2008**, 133.
(31) Petrukhina, N. N.; Kayukova, G. P.; Romanov, G. V.; Tumanyan, B. P.; Foss, L. E.; Kosachev, I. P.; Musin, R. Z.; Ramazanova, A. I.; Vakhin, A. V. Conversion Processes for High-Viscosity Heavy Crude Oil in Catalytic and Noncatalytic Aquathermolysis. *Chem. Technol. Fuels Oils* **2014**, 315.
(32) Ribeiro, A.; Manrique, Y. A.; Lopes, J. C. B.; Dias, M. M.; Barreiro, M. F. Development of water-in-oil Pickering emulsions from sodium oleate surface-modified nano-hydroxyapatite. *Surf. Interfaces* **2022**, *29*, No. 101759.
(33) Petersen, S.; Ulrich, J. Role of Emulsifiers in Emulsion Technology and Emulsion Crystallization. *Chem. Eng. Technol.* **2013**, *36* (3), 398−402.
(34) Farooq, A.; Shafaghat, H.; Jae, J.; Jung, S. C.; Park, Y. K. Enhanced stability of bio-oil and diesel fuel emulsion using Span 80 and Tween 60 emulsifiers. *J. Environ. Manage* **2019**, *231*, 694−700.
(35) Zhang, L.; Liu, R.; Yin, R.; Mei, Y. Upgrading of bio-oil from biomass fast pyrolysis in China: A review. *Renewable and Sustainable Energy Reviews* **2013**, *24*, 66−72.
(36) Lin, B.-J.; Chen, W.-H.; Budzianowski, W. M.; Hsieh, C.-T.; Lin, P.-H. Emulsification analysis of bio-oil and diesel under various combinations of emulsifiers. *Applied Energy* **2016**, *178*, 746−757.
(37) Martin, J. A.; Mullen, C. A.; Boateng, A. A. Maximizing the Stability of Pyrolysis Oil/Diesel Fuel Emulsions. *Energy Fuels* **2014**, *28* (9), 5918−5929.
(38) Li, Q.; Wang, X.-D.; Li, Q.-Y.; Yang, J.-J.; Zhang, Z.-J. New Amphiphilic Polymer with Emulsifying Capability for Extra Heavy Crude Oil. *Ind. Eng. Chem. Res.* **2018**, *57* (49), 17013−17023.
(39) Cao, Y.-B.; Zhang, L.-L.; Xia, D.-H. Catalytic aquathermolysis of Shengli heavy crude oil with an amphiphilic cobalt catalyst. *Petroleum Science* **2016**, *13* (3), 463−475.
(40) Guo, R.; Fu, W.; Qu, L.; Li, Y.; Yuan, W.; Chen, G. Methanol-Enhanced Fe(III) Oleate-Catalyzed Aquathermolysis of Heavy Oil. *Processes* **2022**, *10* (10), 1956.
(41) Tong, J.; Han, X.; Wang, S.; Jiang, X. Evaluation of Structural Characteristics of Huadian Oil Shale Kerogen Using Direct Techniques (Solid-State 13C NMR, XPS, FT-IR, and XRD). *Energy Fuels* **2011**, *25* (9), 4006−4013.
(42) Wang, H.; Hamilton, M.; Rempel, G. L. Hydrogenation of Sodium Oleate in Aqueous Emulsion with the Hoveyda−Grubbs Second-Generation Catalyst. *Org. Process Res. Dev.* **2016**, *20* (7), 1252−1257.
(43) Mullins, O. C. The Modified Yen Model. *Energy Fuels* **2010**, *24* (4), 2179−2207.
(44) Choudhury, R.; Gupta, U. N.; Waanders, F. B.; Saikia, B. K. A multi-analytical study on the sulphur components in some high sulphur Indian Tertiary coals. *Arabian J. Geosci.* **2016**, *9* (2), 100.
(45) Struis, R. P. W. J.; Schildhauer, T. J.; Czekaj, I.; Janousch, M.; Biollaz, S. M. A.; Ludwig, C. Sulphur poisoning of Ni catalysts in the SNG production from biomass: A TPO/XPS/XAS study. *Applied Catalysis A: General* **2009**, *362* (1), 121−128.


https://doi.org/10.1021/acsomega.4c02022
*ACS Omega* 2024, 9, 17681−17690

(46) Schmidts, T.; Schlupp, P.; Gross, A.; Dobler, D.; Runkel, F. Required HLB Determination of Some Pharmaceutical Oils in Submicron Emulsions. *J. Dispersion Sci. Technol.* **2012**, *33* (6), 816−820.
(47) Gore, A. J.; Bhagwat, S. S.; Mhaskar, S.; Saxena, S. Determination of required HLB value and emulsifiers for the preparation of water in coconut oil emulsions for application in food process industries. *J. Dispersion Sci. Technol.* **2023**, *44* (8), 1363−1370.



https://doi.org/10.1021/acsomega.4c02022
*ACS Omega* 2024, 9, 17681−17690